Planar Multilayer Circuit Quantum Electrodynamics

Uday Mathur
Department of Physics, Indian Institute of Technology (BHU), Varanasi
Supervisor: Dr. Rajeev Singh

1 Introduction

Circuit Quantum Electrodynamics (cQED) has advanced the fundamental study of light-matter interactions, particularly the interaction between superconducting qubits and microwave photons. It has emerged as a promising platform for quantum information processing and quantum optics experiments. cQED has been developed using two primary approaches: fully planar (2D) circuits, which leverage the precision and scalability of microfabrication technologies, and 3D circuits, which utilize machined cavities offering superior coherence times. Here I demonstrate lithographically patterned qubits and resonators arranged in multiple planes separated by vacuum gaps, designed to store and confine electromagnetic energy effectively.

In this report, we are harnessing the power of Circuit QED by introducing microwave circuit architecture borrowed from high-Q 3D resonators in quantum regime and planar microfabricated (2D) resonators. We are demonstrating a "2.5D Whisper-gallery mode resonator qubit system" by using the aperture concept in the conducting boundary of the resonator for greater electromagnetic energy confinement to have better coherence time. The device has been replicated and inspired by the research papers. [1] [2]

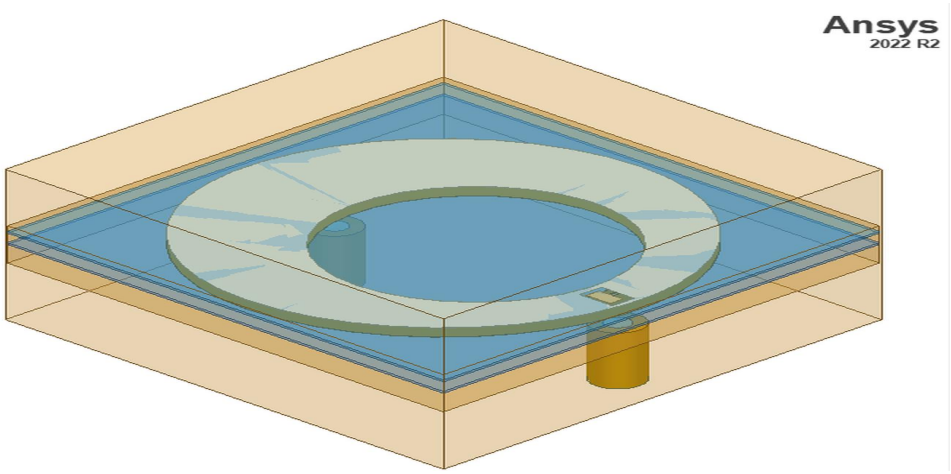

Figure 1: Photograph of the qubit-resonator system (planar whisper-gallery mode resonator with aperture transmon). Two sapphire substrate layers (Al_2O_3): blue, Thin-film aluminum layers: beige, waveports: golden and 3D cavity: semi-orange

2 Device Design

The device comprises a qubit-resonator system enclosed within a high-Q vacuum 3D metal cavity ($20.1mm \times 20.1mm \times 10.1mm$). The resonators are constructed using thin-film aluminum in a multiplanar configuration, with two sapphire chips serving as substrates for each of the two aluminum-patterned rings ($Radius = 9mm$), separated by an electrically thin vacuum gap (0.5mm). The qubit is defined by an aperture ($1mm \times 1.7mm$) carved directly from the conducting boundary of the resonator, with one qubit pad ($0.6mm \times 1.6mm$) situated inside the carved region of the conducting plate ($Thickness = 0.0125mm$) and the other being the plate itself. Additionally, two waveguide ports are defined with a boundary condition at the ends with 50Ω resistance, facilitating the signaling and manipulation of electromagnetic signals.

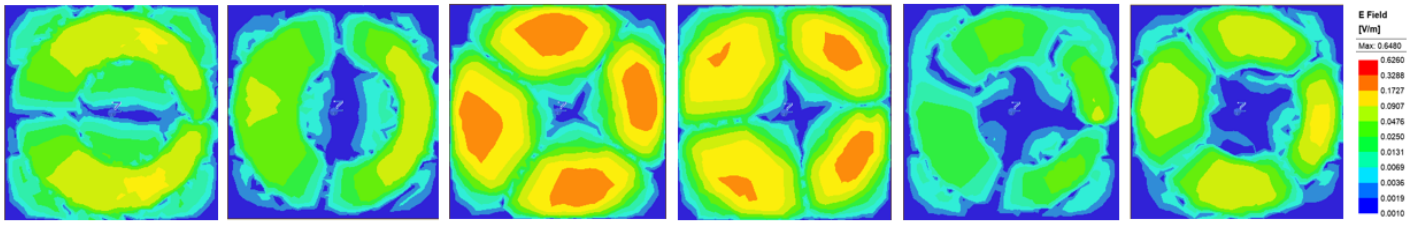

Figure 2: The modal profiles of the resonator-qubit system in Ansys 2022 [4]

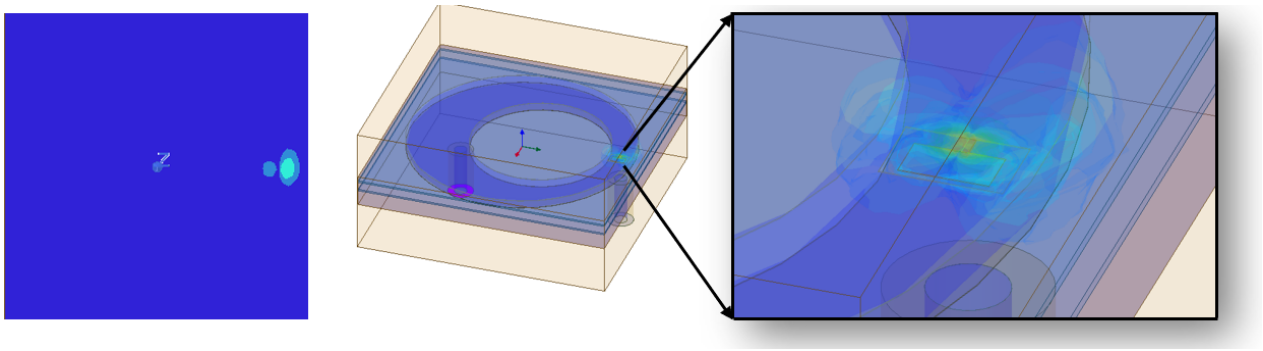

Figure 3: The electromagnetic modal profile of the qubit mode shows that the majority of the modal field interacts with the qubit, with a significant amount of field intensity concentrated around it.

3 Results and Analysis

Fig. 2 represents the modal profiles of the resonator-qubit system. It can be observed that the first two profiles have the same principal mode number ($n_m = \lambda N$) with $N = 2$ denoting the number of lobes, which remain unchanged. However, they differ in their azimuthal mode number (n_ϕ) due to the change in the orientation of the lobes. A similar pattern can be seen in the subsequent four profiles, which also exhibit four lobes ($N = 4$) but differ in azimuthal mode numbers, highlighting the variations in angular symmetry and orientation of the electromagnetic field distribution. These profiles can be extended to six lobes also on further increment of the number of modes. This device implementation is based on

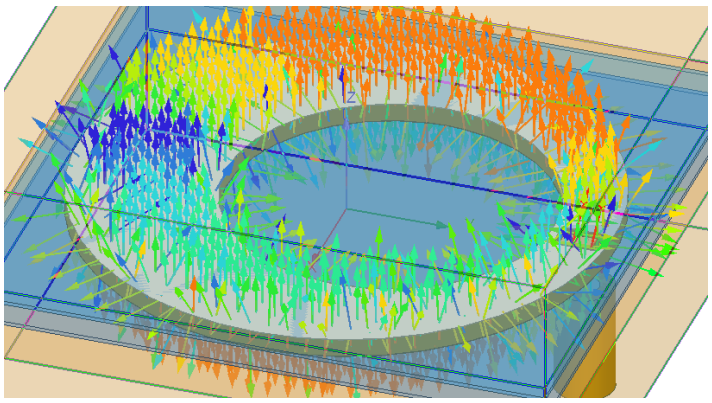

Figure 4: ($D_\parallel$ *and* $D_\perp$) mode profiles

two TEM modes ($D_\parallel and D_\perp$). One of the modes is overcoupled and can be used for readout purposes, while the other can be used for storage. The parallel component of the electric displacement field ($D \parallel$) is a component of D that is tangential to the materials or boundaries in the device.($D_\parallel = \epsilon E_\parallel, \epsilon = 1(vacuum)$). A similarly perpendicular component of the electric displacement field ($D_\perp$) normal to the surface of the conducting plate, where ($D_\perp$) is critical near the qubit, as it defines electric field gradient interacting with the qubit's dipole moment.

For analyzing and extracting the system parameters I have done multiple eigenmode analyses in Ansys [4] with varying qubit position angles and spacing in between the two layers of the device. I varied the qubit position angle in the range from 0 to 180 degrees with steps of 45 degrees. I observed that for each angle other than 0 degrees, the junction has $E_j/\hbar = 8.173076$ GHz. while after considering junction capacitance and all the geometric capacitances, the value of junction charging energy is $E_C/\hbar = 9.685115$ GHz which is greater than the junction inductive energy $E_j/E_c < 1$. Thus, in this condition, the qubit is more prone to greater charge sensitivity, which can adversely affect the qubit coherence. However at $\theta = 0$ the ratio becomes a little bit greater than before with $E_J/\hbar = 16.346151$ GHz and $E_C/\hbar = 9.685115$ GHz, thus we have ($E_J/E_C > 1$). Here are the system parameters that I have extracted using pyEPR [5]for a particular case mentioned below.

Table 1: Data Extracted from the pyEPR Analysis

Parameter	**Value**	**Parameter**	**Value**
Angle (θ)	0	**Spacing**	0.5 mm
$E_J/\hbar$	6.346151 GHz	$E_C/\hbar$	9.685115 GHz
$w_q/2\pi$	9.67 GHz	p_{j_1}	0.240949
$w_{D_\perp}/2\pi$	11.7537 GHz	$Q_{D_\perp}$	4.1958×10^4
$w_{D_\parallel}/2\pi$	11.9915 GHz	$Q_{D_\parallel}$	8.2645×10^7

λ : It is an arbitrary proportionality constant, but couldn't be identified through ANSYS

4 Inference

From the data above, it is clear that the quality factor for the $D_{\parallel}$ mode is quite high, with $Q_{D_{\parallel}} > 10^6$. This encourages us to consider this mode optimistically for our storage application. The $D_{\parallel}$ component is tangential to the conductive surface boundary, which aligns with the qubit's dipole moment, and facilitates a weak but precise interaction that helps preserve the qubit's coherence while allowing for effective quantum state storage. The high-quality factor of storage mode enhances quantum information retention, resulting in improved high relaxation time T_1 and T_2 values. This enables the demonstration of cat state formation and stability analysis through Wigner function plots.

On the other hand, the quality factor of the $D_{\perp}$ mode is comparatively lower than that of $D_{\parallel}$ ($Q_{D_{\perp}} \sim 10^4$). Since Q_{ext} quantifies the energy exchange with the environment, a lower Q_{ext} indicates stronger coupling, meaning that $D_{\perp}$ dissipates energy to the environment more quickly, which is desirable for fast and efficient readout. This enables us to use $D_{\perp}$ as a readout mode.

5 Proposal for Modifications

The design can be further optimized by increasing the inner pad width, which enhances the capacitance between the inner pad and the conducting plate, thereby reducing E_C. This results in an overall increase in the ratio E_J/E_C, making the transmon more robust and less sensitive to charge noise. However, this comes with a trade-off between robustness and anharmonicity.

We can also design the entire device structure in a cylindrical manner. This offers two benefits: first, the reduction of noise due to sharp edges; second, it enables symmetry with the electromagnetic mode pattern in the device.

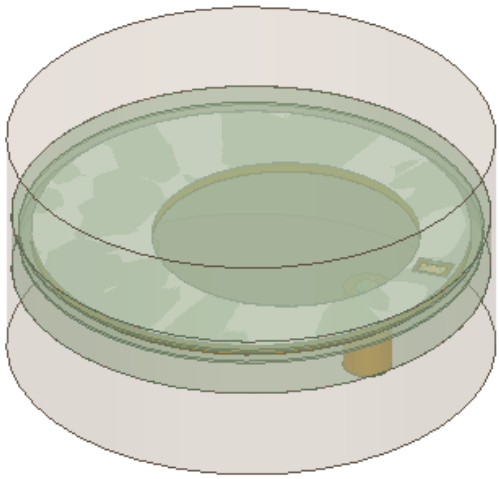

Figure 5: cylindrical designed device structure

References

[1] Z. K. Minev, I. M. Pop, and M. H. Devoret, "Planar Superconducting Whispering Gallery Mode Resonators," *Appl. Phys. Lett.*, vol. 103, p. 142604, 2013. [Online]. Available: `https://doi.org/10.48550/arXiv.1308.1743`.

[2] Minev, Z. K., K. Serniak, I. M. Pop, Z. Leghtas, K. Sliwa, M. Hatridge, L. Frunzio, R. J. Schoelkopf, and M. H. Devoret, "Planar multilayer circuit quantum electrodynamics," *ArXiv:1605.09077*, 2016. [Online]. Available: `https://arxiv.org/pdf/1509.01619`.

[3] Qiskit Metal: An open-source framework for quantum device design, IBM Research, 2021. [Online]. Available: `https://qiskit-community.github.io/qiskit-metal/`. [Accessed: 21-Sep-2024].

[4] "Ansys HFSS: High-Frequency Electromagnetic Field Simulator", Ansys Inc., 2021. [Online]. Available: `https://www.ansys.com/products/electronics/ansys-hfss`.

[5] Minev, Z. K., "pyEPR: Python for Energy Participation Ratio", GitHub Repository, 2021. [Online]. Available: `https://github.com/zlatko-minev/pyEPR`.